ACCSCIENCE PUBLISHING

Asian Journal of Water, Environment and Pollution

ORIGINAL RESEARCH ARTICLE

Assessment of water quality in the coastal wetland of Kalathas, Crete, Greece: A local-scale wetland at high risk

Despoina-Eleni Zacharioudaki[1], Ioannis Fitilis[1], Eleni Kokinou[2], and Melina Kotti[1]*

[1]Department of Electronic Engineering, School of Engineering, Hellenic Mediterranean University, Chania, Crete, Greece

[2]Department of Agriculture, School of Agricultural Sciences, Hellenic Mediterranean University, Heraklion, Crete, Greece

Abstract

Coastal wetlands are highly dynamic ecosystems where natural processes and anthropogenic pressures interact to control water quality. This study evaluates the physicochemical characteristics, nutrient dynamics, photosynthetic pigments, and fluorescence properties of the Kalathas coastal wetland in Crete, Greece, over one year (2022), providing an integrated assessment of its environmental status. The wetland exhibited alkaline conditions and pronounced spatial variability associated with marine intrusion. Among nutrients, silicon showed a strong and consistent positive relationship with chlorophyll a, indicating its key role in regulating phytoplankton biomass. In contrast, total hardness was negatively associated with chlorophyll a, suggesting that increased ionic strength may limit biological productivity. A strong negative relationship between chloride concentrations and fluorescence emission intensity was also observed, consistent with fluorescence quenching under high ionic conditions. Overall, water quality in the wetland appears to be controlled by the combined influence of geological background, marine intrusion, and localized anthropogenic inputs. These findings provide a robust baseline for this understudied ecosystem and highlight the need for continuous monitoring to support effective management and conservation.

Keywords: Coastal wetland; Laser-induced fluorescence; Nutrients; Photosynthetic pigments; Water quality

***Corresponding author:**
Melina Kotti
(kotti@hmu.gr)

Citation: Zacharioudaki D-E, Fitilis, I, Kokinou E, Kotti M. Assessment of water quality in the coastal wetland of Kalathas, Crete, Greece: A local-scale wetland at high risk. *Asian Journal of Water, Environment and Pollution.* doi: 10.36922/AJWEP026130082

Received: March 23, 2026

Revised: May 8, 2026

Accepted: May 8, 2026

Published online: May 26, 2026

1. Introduction

The definition for wetlands according to the Ramsar Convention is: "Wetlands are natural or artificial, permanent or temporary areas of marsh, bog, peatland, or water containing standing or flowing fresh, brackish, or saline water, including marine waters, the depth of which does not exceed six meters at low tide."[1(p245)] One category of wetlands is the coastal wetlands, which are connected to coastal zones. In Greece, 803 (590 natural and 213 artificial) coastal wetlands were recorded; 191 are situated in the southern part of Greece, in Crete (105 natural and 86 artificial). They are protected by either European or national legislation. Although protected, recent studies have shown that many of them are under severe threat due to pressure from human activities and climate change.[2] To our knowledge, the coastal wetland in the present study has not been reported elsewhere. It is known as Kalathas estuary or Kalathorema, and is situated in the prefecture of Chania in northwest Crete. It was designated a landscape of outstanding natural beauty in 1973. In 2012, it was included in the list of small island wetlands protected, among others, by Presidential Decree.[3]

The Presidential Decree specifies protection measures for these wetlands and prohibits activities such as drainage and drainage works, as well as interventions that may change the hydrological regime, including drilling and water pumping, unless they intend to maintain the wetland. Unfortunately, the current condition is not the expected one, as it has obvious degradation signs (symptoms) such as shrinkage of the bed, decline of depth, intense algal bloom, and litter. Due to its proximity to a highly touristic beach and its small area, it does not attract proper concern. These facts must not overcome its importance as an ecosystem. There is a mandatory need for the authorities to protect it, as its decline can be fatal and irreversible.

The Water Framework Directive (2000)[4] is considered the main law for the protection of water bodies in Europe. The Directive establishes the physicochemical and biological parameters for assessing water quality. Examples of physicochemical parameters commonly monitored include pH, electrical conductivity, total hardness, chloride, and nutrients. Biological parameters include bacteria, algae, and viruses.[5] Photosynthetic pigments, particularly chlorophylls, are also biological indicators, as they are components of plants and types of phytoplankton, and are the basic players in photosynthesis.[6] The parameters should be monitored regularly as they change rapidly due to constant interventions.[7]

For the characterization of organic material in water bodies, fluorescence spectrometry has proven to be a powerful tool. Organic material is a complex mixture of organic, aromatic, and aliphatic compounds with functional groups such as carboxyl, hydroxyl, phenol, carbonyl, amine, and thiol.[8] It can be analyzed either with conventional spectrometers[9–11] or with laser-induced fluorescence (LIF).[12,13] The high sensitivity of LIF is its advantage, but it lacks the ability to generate an excitation-emission matrix.

This study aims to assess the water quality and underlying biogeochemical processes of the Kalathas coastal wetland in Crete, Greece, through the analysis of physicochemical parameters, nutrients, photosynthetic pigments, and fluorescence properties over a one-year period. It investigates the spatial and temporal variability of these parameters and identifies key environmental factors influencing phytoplankton biomass. In addition, LIF was used to estimate dissolved organic matter and characterize water quality. A multivariate statistical analysis was performed to assess correlations between all parameters.

2. Materials and methods

2.1. Site description

The Kalathas coastal wetland is situated in the prefecture of Chania in the northwest of Crete, Greece (Figure 1A). The wetland was designated by the World Wide Fund for Nature Greece[14] under the code GR434KRI187 in 2013. The stream contains brackish water with a permanent flow regime and has an area of 0.6 ha. The plant species include *Ammophila arenaria*, *Pancratium maritimum*, *Eryngium maritimum*, *Juncus* sp. (dominant), *Phoenis* sp., and *Tamarix* sp.

From communication with inhabitants, it is known that the wetland was at least five times larger than it is nowadays, but was drained for the construction of a main road. It has also been heavily affected by sand and gravel extraction. The main road, constructed many years ago, divides the wetland into two parts. The smaller part is closer to the famous Kalathas beach. Most months of the year, especially in summer, people primarily use the beach for recreational activities and occasional water sports. The larger part is parallel to a side road. A sewage pumping station and an old aggregate mining quarry are located on the other side of this road, almost at the beginning of the wetland. Rarely, some agricultural activities (grazing) are observed, mostly in winter. Five sites were sampled before (S1–S5) and one after (S6) the crossing. S1 is the shallowest site of all and closest to the sewage pumping station (Figure 1B).

There is a lack of hydrological data available about the area. As far as the geological data are concerned, the oldest geological formation in the study area is Triassic–Cretaceous limestones (Figure 2A)[15,16], which are compact, white–grey to bluish, microcrystalline to aphanitic, mostly with rudist fragments, sometimes breccias in places, dolomitized, and strongly karstified. Deposits of terra rossa from the Quaternary are also present in karst depressions. Terra rossa is a reddish clayey to silty–clayey soil that is particularly common in the Mediterranean area and covers limestone and dolomite in the form of a discontinuous layer with a thickness of a few cm to several m. The rest of the area is covered by Miocene marls and marly limestones. The marls are yellow–brown to white–yellow and often alternate with layers of marly sandstone and platy limestones containing fossils of marine molluscs. The marly limestones are compact, white–yellow to white–

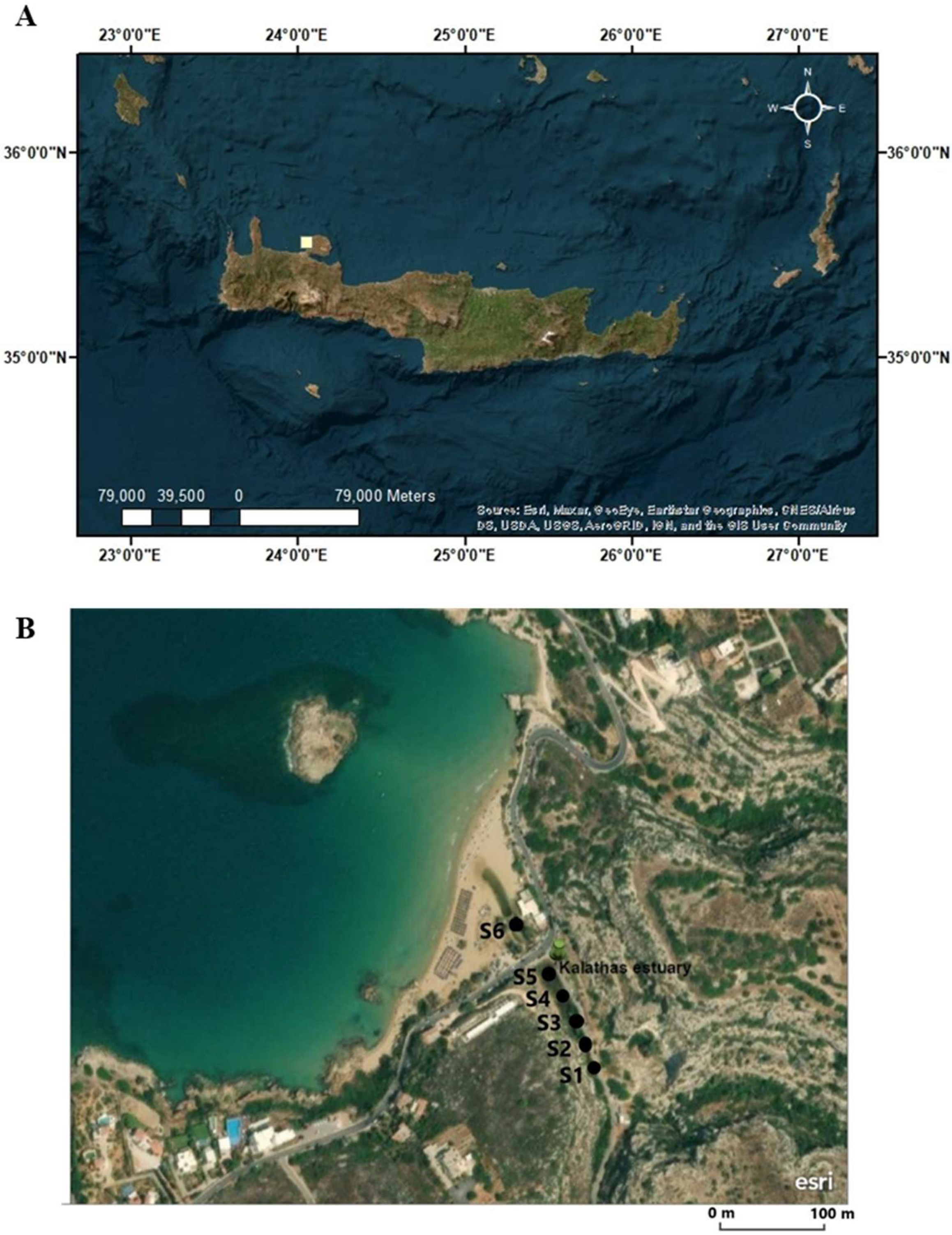

Figure 1. Kalathas Wetland. (A) Google Earth satellite map showing the location of Kalathas Bay (yellow rectangle) in the northwest of Crete, Greece, in the Eastern Mediterranean Sea. (B) Google Earth satellite map showing the locations of the water samples for 2022.

grey, and contain sea fossils.

Furthermore, to examine the proportion and variation of soil sealing in the extensive region of Kalathas Wetland (Figure 2B), we used the imperviousness density (IMD) from Copernicus (https://land.copernicus.eu/pan-european/high-resolution-layers/imperviousness/status-maps; accessed on September 28, 2023). The IMD data were available at a spatial resolution of 10 m (2018) and adjusted to the national coordinate system (GGRS87/Greek grid) to ensure compatibility with the other datasets used in this study. These data were then reclassified. IMD ranged from 1% to 100% and was assessed using a semi-automatic classification based on calibrated normalized difference vegetation index values. The spatial arrangement of the data was presented using a Geographic Information System. As shown in Figure 2B, Kalathas Stream crosses an area with high IMD, ranging from 48% to 100%.

2.2. Meteorological conditions

The climate in Chania is typical Mediterranean. The weather is temperate and mild, with very hot and dry summers and mild, wet, and windy winters. The sunshine is approximately 300 days a year. Autumns and springs are warm seasons. During the survey, January and March 2022 were the coldest months, and July 2022 was the hottest month. In April 2022, temperatures suddenly increased. Many rainfall events occurred from January to March 2022

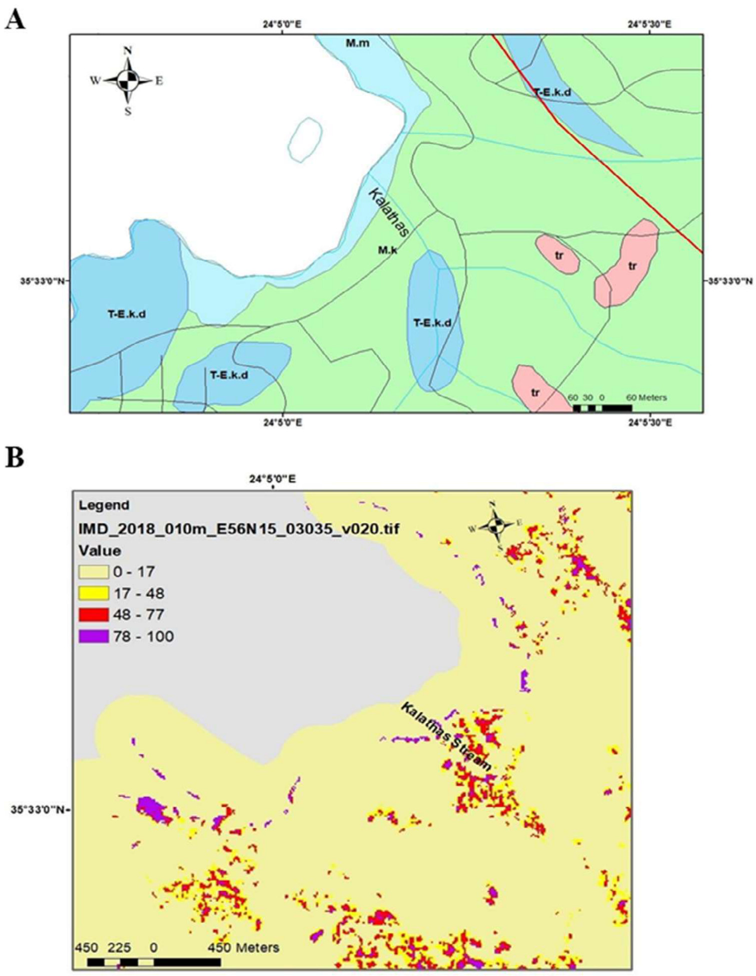

Figure 2. Geological background and imperviousness density distribution in Kalathas Wetland. (A) Geological map of Kalathas Wetland.[15,16]
Map symbols: Black line: Road network; Blue line: Hydrographic network; M.k: Miocene marly limestones; M.m: Miocene marls; Red line: Geological fault; T-E.k.d: Triassic–Cretaceous limestones; tr: Deposits of Quaternary terra rossa. (B) Distribution of imperviousness density (IMD; %) in Kalathas Stream.

and from September to December 2022, with October having extreme storms. In addition, sporadic rainfall events happened during May and September 2022. The data were collected from the nearest and most representative meteorological stations. The year of the study was among the wettest years for Chania. Furthermore, 2022 was characterized by a strong and prolonged La Niña event, a state of the El Niño–Southern Oscillation (ENSO) phenomenon.

2.3. Sampling collection and storage

The study was conducted from January to December 2022. Surface water samples were collected using a rope and a bucket at six stations (S1–S6) along Kalathas Wetland once per month. Five sites were selected in the larger part and one in the smaller part of the wetland, near the sea, as shown in Figure 1B. The samples were stored in 1-L polytetrafluoroethylene (PTFE) bottles that were pre-cleaned with tap water, deionized water, 5% hydrochloric acid (HCl) solution, tap water, and finally deionized water. If they were not to be analyzed within 24 h, they were stored at 4 °C in the dark. All the analyses were completed within three days.

2.4. Laboratory analysis

2.4.1. Chemical analysis

All measurements were performed using standard analytical methods.[17] All chemical reagents used were of analytical grade and were purchased from Sigma-Aldrich (United States [US]) unless otherwise stated. The determination of physicochemical parameters, including pH, electrical conductivity, and salinity, was carried out using a multiparameter probe. Total hardness and chloride were determined titrimetrically using ethylenediaminetetraacetic acid (EDTA) and silver nitrate ($AgNO_3$), respectively. Ammonium was determined after filtration of the sample using the spectrophotometric method (U-2001, HITACHI, JAPAN) of Nessler (Labkem, Spain) (limit of detection [LOD] = 0.005 mg/L). Nitrate was determined by subtracting the absorbance at 275 nm from the absorbance at 220 nm (LOD = 0.020 mg/L). For phosphate, the spectrophotometric molybdenum blue method was used, with the reagents concentrated sulfuric acid and ascorbic acid purchased from Honeywell (US) and Labkem, respectively (LOD = 0.003 mg/L). For silicate, the same method as for phosphate was used, except that oxalic acid (Labkem) was added to suppress interference from phosphate (LOD = 0.007 mg/L). The photosynthetic pigments chlorophyll a (chl a), chlorophyll b (chl b), chlorophyll c (chl c), and carotenoids were detected using the spectrophotometric trichromatic method after filtration of the samples with 0.45 μm filters and extraction with 90% acetone (Honeywell).

2.4.2. Fluorescence measurements

For the fluorescence measurements, the 4th harmonic of a neodymium-doped yttrium aluminum garnet pulsed laser at 266 nm was used (Q-SMART 850, QUANTEL, FRANCE). The output pulse energy was approximately 2.5 mJ/pulse at a repetition rate of 10 Hz and a pulse width of 6 ns. The experimental setup is depicted in Figure 3, and the operational parameters are summarized in Table 1. Prior to measurements, all water samples were allowed to reach room temperature. The water samples were placed in a quartz cell of 1 cm path length. The sample was excited by the laser beam, and the fluorescence emission was collected at a path perpendicular to the excitation beam by a pair of lenses (UV-fused silica) to an optical fiber (QP100–2–UV–VIS, Ocean Optics, US). The collected fluorescence signal was recorded by a spectrometer (HR4000CG–UV–NIR; Ocean Optics) in the wavelength range of 200–1,000 nm. The integration time was set to 10 s, with the signal accumulated from 100 laser-pulse excitations at a repetition rate of 10 Hz. Ambient light was kept to a minimum, and a reference signal of a deionized sample was removed from the signal of the sample's measurement.

A calibration curve was created to quantify fluorescence signals. The standard compound was quinine sulfate dihydrate dissolved in 0.1 N H_2SO_4. Quinine sulfate dihydrate is the most suitable compound for calibration, as it has a spectrum similar to that of the natural fluorescent compounds. When excited at 250 nm or 350 nm, it shows a fluorescence maximum (emission wavelength) at 450 nm.[18]

The calibration data are shown in Table 2. The precision of the method, expressed as the percentage relative standard deviation, was determined by performing six measurements of a standard sample, and the LOD was calculated from the standard deviation of 20 blank-sample measurements.

Table 1. Operational parameters for the laser-induced fluorescence measurements

Parameter	Value
Wavelength	266 nm
Laser power	7.37–9.96 mJ (average 8.3 mJ)
Pulse duration (FWHM)	6 ns
Pulse frequency	10 Hz
Recording spectrum	200–1,000 nm
Optical resolution	<1 nm
Recording time	10 s

Abbreviation: FWHM: Full width at half maximum.

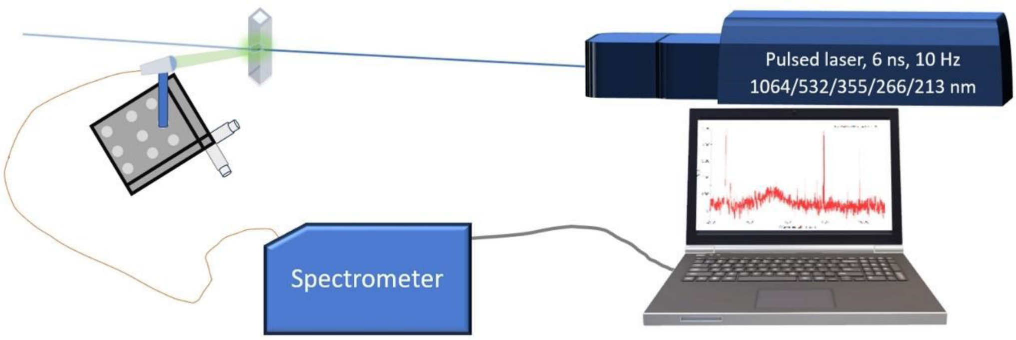

Figure 3. Setting for laser-induced fluorescence measurements. The 4th harmonic of a neodymium-doped yttrium aluminum garnet pulsed laser at 266 nm excites the sample in a quartz cuvette. The fluorescence emission light is collected perpendicular to the excitation path and guided into an optical fiber. Translation stages adjust the collection optics to maximize the recorded signal. The light is directed to the entrance of a spectrometer, where the spectrum from 200 nm to 1,000 nm is recorded.

Table 2. Calibration data, repeatability, and method detection limit of the studied compounds

Parameter	Value
Equation	y = 3.475x + 31.248
R^2	0.9983
Range	0.41–51.25 ppm quinine sulfate
LOD	0.37 ppm
RSD (%)	3.6

Abbreviations: LOD: Limit of detection; RSD: Relative standard deviation.

The concentrations of the organic fluorescents are determined from the intensities at the peak wavelength. The fluorescence intensities were converted to quinine sulfate units (ppm qs) to allow easy comparison with fluorescence results from other studies.

2.5. Statistical analysis

Statistical analyses were performed using Microsoft Excel (US) and JASP 0.19.3 (JASP Team, Netherlands). Relationships among physicochemical parameters, nutrients, photosynthetic pigments, and fluorescence indices (pH, chlorides, hardness, $N\text{-}NH_4$, $N\text{-}NO_3$, $P\text{-}PO_4$, Si, chl a, chl b, chl c, carotenoids, and emission at 480–490 nm) were examined using both Pearson's correlation coefficient (r) and Spearman's rank correlation coefficient (ρ).

Pearson's correlation coefficient was used to quantify the strength and direction of linear relationships between variables, while Spearman's correlation coefficient was applied as a non-parametric alternative to assess monotonic relationships and to evaluate the robustness of the results under non-normal data distributions. Spearman's coefficient is based on ranked data and is less sensitive to skewness and outliers, making it particularly suitable for environmental datasets where normality assumptions are often violated. When the values of r range from −1 to −0.75 and from 0.75 to 1, the correlation of the two variables is very strong. If the r value falls within the range of −0.75 to −0.5 and from 0.5 to 0.75, the two variables reveal a moderate correlation. When it ranges from −0.5 to −0.25 and from 0.25 to 0.5 or from −0.25 to 0.25, it indicates a weak or no linear correlation between the two variables, respectively.

The p-value indicates the probability of obtaining a Pearson's correlation coefficient as extreme as the observed value, assuming that there is no linear relationship between the two variables in the population. It is used to assess whether the observed correlation is statistically significant at a chosen significance level (e.g., 0.05 or 0.01). In the present case, the p-value was set at 0.05. A p-value less than this threshold suggests that the correlation coefficient is statistically significant, while a greater value indicates that the correlation coefficient is not statistically significant.

Outliers were identified using the interquartile range (IQR) method, where values outside 1.5 × IQR (Q1 − 1.5 × IQR and Q3 + 1.5 × IQR) were considered outliers. These observations were removed at the observation level to ensure consistency across variables in the multivariate analysis.

Due to values that were not detectable and thus considered missing, the effective sample size varied across parameters, and correlations were computed using pairwise complete observations. In addition, several variables exhibited non-normal distributions even after outlier removal; therefore, the correlation analysis is considered exploratory.

3. Results

3.1. Descriptive statistics

Tables A1 and A2 present the descriptive statistics of the measured variables before and after outlier removal, respectively. Outliers were identified and removed at the observation level, resulting in a more consistent dataset for subsequent multivariate analysis. Following outlier removal, a general reduction in variability was observed across several parameters, as reflected in lower standard deviations and narrower IQRs. In addition, the distributions of some variables became more symmetric; however, several parameters, particularly N-NH_4, total hardness, and carotenoids, still exhibited positive skewness, indicating that non-normality persists even after data cleaning.

The number of observations (*n*) varies among variables in both Tables A1 and A2. This variation is attributed to missing values in specific measurements rather than additional filtering procedures and therefore reflects the inherent structure of the dataset. As a result, the statistical analyses were based on pairwise complete observations.

The physicochemical parameters (Tables A1 and A2) indicate that the wetland is characterized by alkaline conditions, with pH values mostly above 7.5. Chloride concentrations and total hardness exhibited relatively high mean values and wide ranges, reflecting strong spatial variability, particularly S6, which is likely influenced by marine intrusion. This spatial heterogeneity is also evident in the high variability of salinity and conductivity in the original dataset.

Nutrient concentrations showed notable variability. Ammonium (N-NH_4) presented high skewness and variability, suggesting the presence of sudden inputs or localized processes such as organic matter degradation. In contrast, nitrate (N-NO_3) and phosphate (P-PO_4) displayed more stable distributions with lower skewness values after outlier removal. Silicon exhibited moderate variability and remained one of the most abundant nutrients in the system.

Photosynthetic pigments also showed considerable variation. Chl a exhibited relatively high mean concentrations, consistent with eutrophic conditions, while chl b and chl c displayed similar ranges but slightly different variability patterns. Carotenoids showed strong positive skewness, indicating occasional high concentration events. These patterns suggest dynamic biological responses to environmental conditions within the wetland.

Fluorescence emission intensities (480–490 nm) exhibited moderate variability and slight negative skewness, suggesting relatively stable background levels of dissolved organic matter, with occasional lower intensity values.

Salinity and electrical conductivity were excluded from the correlation analysis not only due to their skewness but also because they exhibited strong spatial gradients driven by marine influence, which could dominate the correlation structure and obscure relationships among the remaining variables. However, their temporal and spatial trends are presented descriptively in Figure 4B,E.

3.2. Variations in physicochemical parameters

Figure 4 shows the results of the physicochemical parameters of all samples collected during the one-year survey. There were no spatial variations in pH, only temporal variations. The lowest pH values were observed in January, while the highest values were recorded in February and July 2022 (Figure 4A). Most pH values were above 7.5, indicating that the Kalathas water body is alkaline.

Salinity had the highest value at S6 in April 2022 and the lowest in September 2022, while at S1–S5, the lowest values were in March 2022 (Figure 4B). From August to December 2022, almost the same salinity values were observed at all stations. Chloride concentrations showed the same seasonal fluctuations at all stations (Figure 4C). S6 showed substantially higher concentrations compared to the other stations. The highest chloride values were observed in July 2022, the month with the highest temperature.

Total hardness (Figure 4D) showed a similar trend to the salinity. The highest value was also observed at S6, and a smaller increase was observed in February 2022 at the other stations. Electrical conductivity values in the Kalathas Wetland followed similar changes at S1–S5, while the opposite was true at S6 (Figure 4E). From August to December, all the stations had similar conductivity values.

3.3. Variations in nutrients nitrogen, phosphorus, and silicon contents

Figure 5 shows the fluctuations in the concentrations of nutrients N-NH_4, N-NO_3, P-PO_4, and silicon. S6 exhibited higher N-NH_4 concentrations than the other stations, especially during April and August 2022 (Figure 5A). These elevated NH_4 concentrations can be attributed to increased organic matter degradation; however, dissolved oxygen was not measured in this study. S5 also consisted of high ammonium concentrations. S5 and S6 were close to each other and to the sea. In contrast, N-NO_3 was lower at S6 (Figure 5B). The highest N-NO_3 values for S1–S5 were observed in January 2022. From August until December

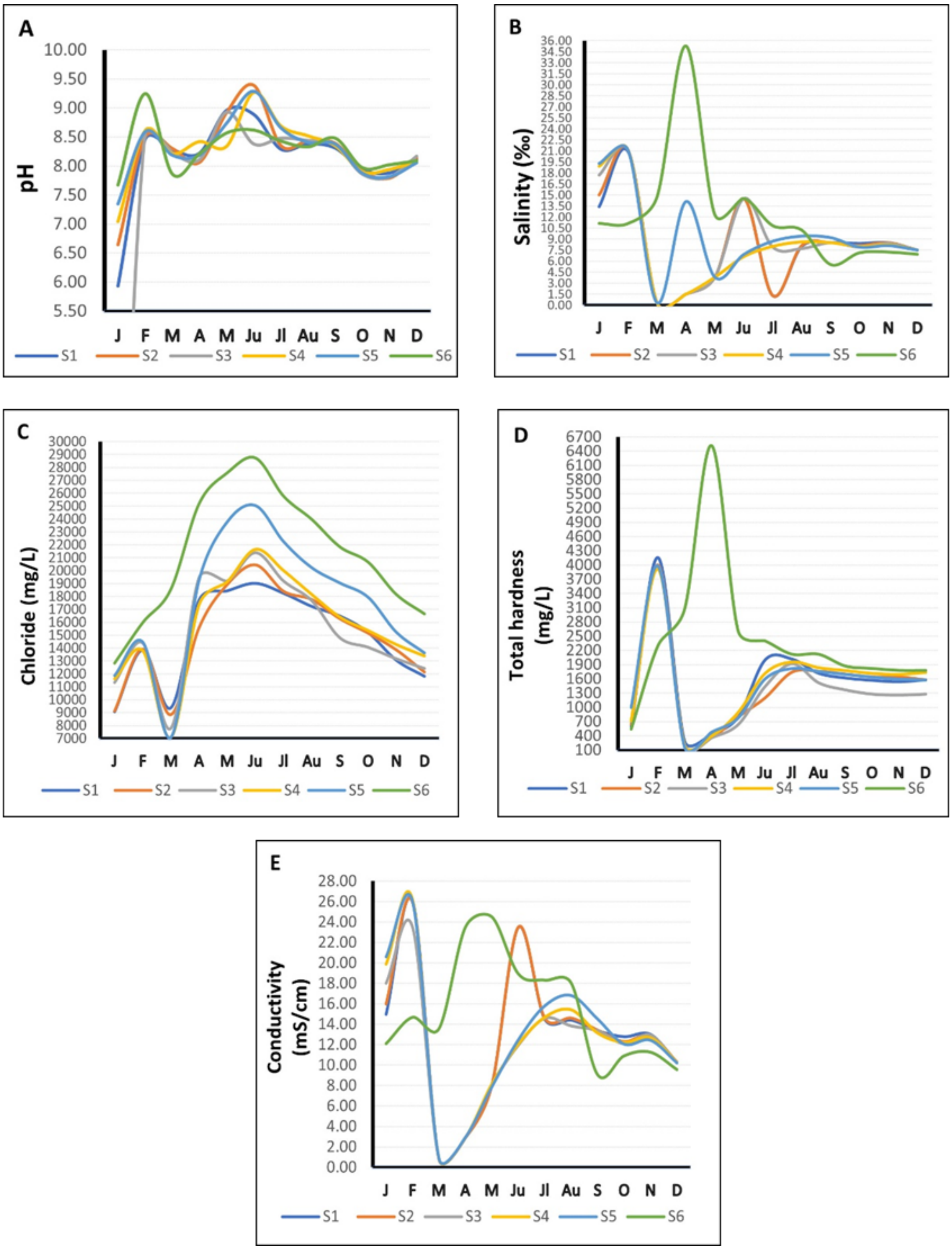

Figure 4. Monthly measurements of physicochemical parameters from January to December 2022 (*x*-axis) at the six sampling stations (S1–S6) at Kalathas Wetland: (A) pH, (B) salinity, (C) chloride, (D) total hardness, and (E) electrical conductivity.

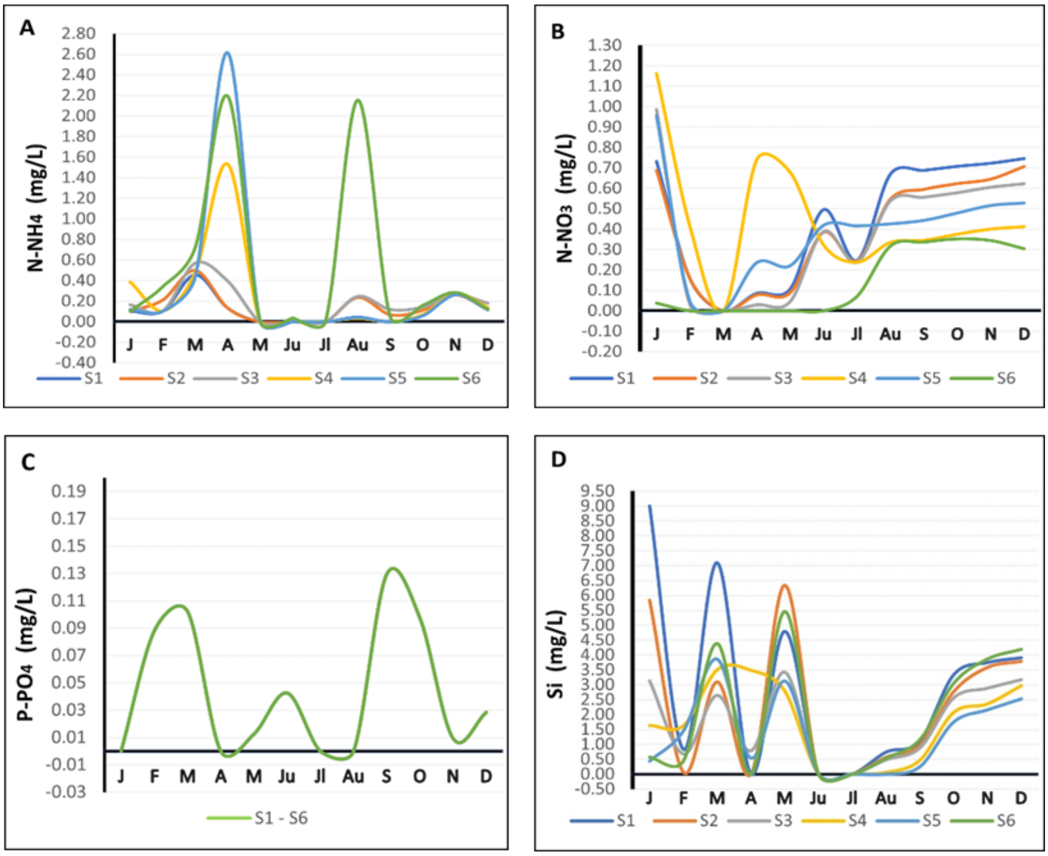

Figure 5. Monthly measurements of nutrients from January to December 2022 (x-axis) at S1–S6 at Kalathas Wetland: (A) N-NH_4, (B) N-NO_3, (C) P-PO_4, and (D) Si.

2022, the same trend was observed for all stations. N-NO_3 generally occurred in low concentrations. From Tables A1 and A2, it is clear that the two nitrogen species exhibited comparable concentrations, with NH_4 showing greater variability.

The P-PO_4 values were the same at all stations throughout the entire period and fluctuated only monthly (Figure 5C), suggesting a common source or controlling process for phosphates in the wetland. The highest values occurred in September and March 2022, potentially due to rain events and runoff from the pumping station. In February 2022, the value was also high, and it was slightly lower in July 2022. According to the OECD[19] classification system, the wetland is categorized as eutrophic, as the mean value of P-PO_4 was slightly less than 0.1 (Tables A1 and A2). This system uses annual mean values of total phosphorus, chl a, and transparency (measured with a Secchi disk) to classify water systems. The molar ratio of nitrogen-to phosphorus (N:P), as calculated from the mean values of N and P (Tables A1 and A2), was 14.5, indicating either colimitation of N and P or no limitation. Molar ratios between 10 and 17 are found in coastal wetlands that represent a transitional zone for both N and P limitation or no limitation[20,21], less than 10 are found in marine waters where there is N limitation, and higher than 17 are found in freshwater with P limitation.[22]

Silicon varied monthly and to a lesser extent spatially (Figure 5D). S1 had the highest values. This station has the lowest depth. Extremely low silicon concentrations were detected in the summer months, June and July 2022, while higher values were observed in March and May 2022.

3.4. Variations in photosynthetic pigments

The variations in the concentrations of photosynthetic pigments are depicted in Figure 6. Figure 6A shows that chl a varied both spatially and temporally, except in January and February 2022. S4 had lower values than the other stations and very low values from April to September 2022. The mean levels of chl a were high (Tables A1 and A2), indicating that the trophic status of the wetland is eutrophic according to the established OECD (1982) thresholds for chlorophyll levels. Thus, from levels of both

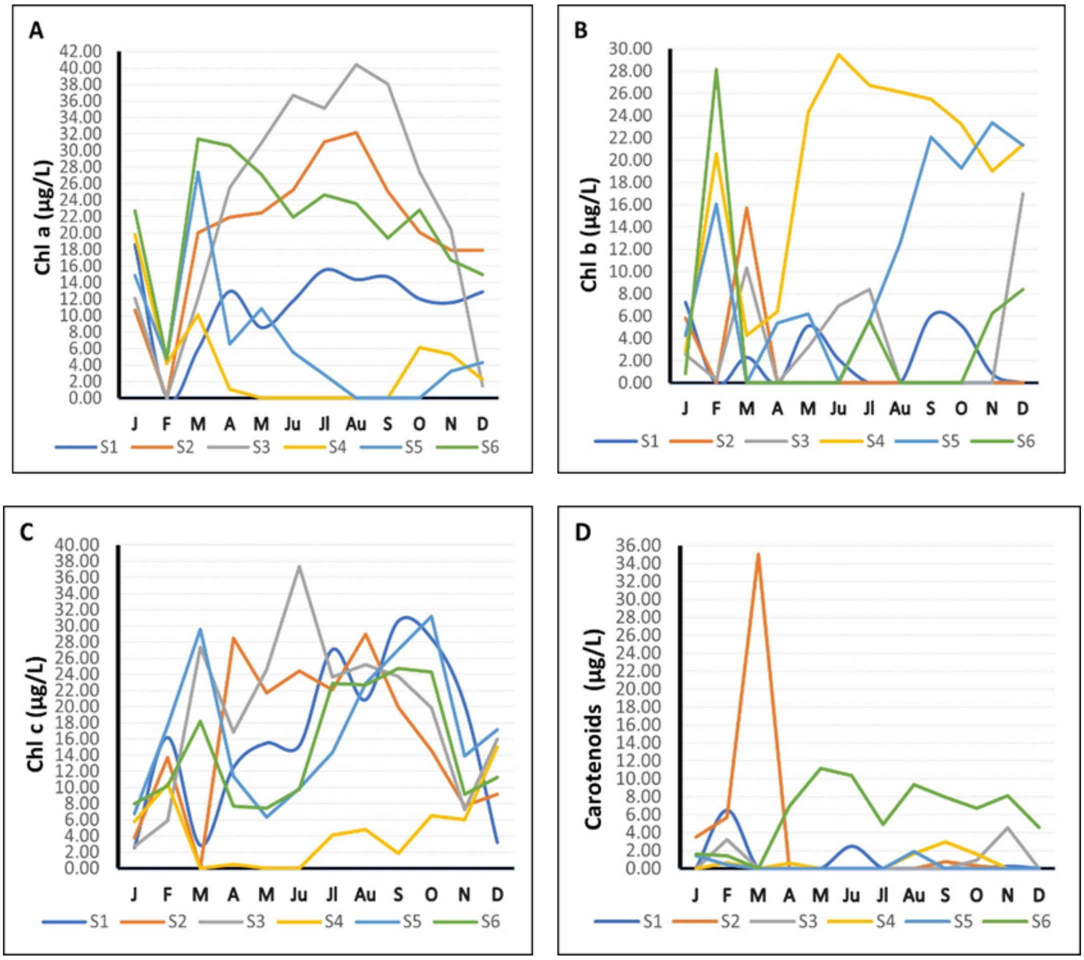

Figure 6. Monthly measurements of pigments from January to December 2022 (*x*-axis) at S1–S6 at Kalathas Wetland: (A) chlorophyll (chl) a, (B) chl b, (C) chl c, and (D) carotenoids.

phosphorus and chl a, it is concluded that the wetland is eutrophic. The highest values of chl a and chl c (Figure 6A,C) were measured at S3, while chl b had the highest value at S4 in July and was higher than at the other stations during most months (Figure 6B). On the other hand, chl b was low at S6 in July 2022 and high in February 2022. The carotenoids fluctuated similarly at all stations (Figure 6D). Higher levels of carotenoids were observed at S6, while S2 showed a clear maximum in March. S6 had lower concentrations of the three chlorophyll species but higher concentrations of carotenoids. From Tables A1 and A2, it is obvious that the mean levels of chl b and chl c were almost the same and slightly higher than the mean level of chl a. The spatial and temporal variations in chlorophyll species are not surprising, as they have been widely documented to be affected by water physical properties, nutrient availability, light penetration, and grazing.[23,24] Carotenoids are less affected by harsh conditions.[25,26]

3.5. Variations in fluorescent compounds

Figure 7 shows two representative emission spectra from different samples excited at 266 nm. The spectra of the two samples were similar.

The Raman line (inelastic scattering of laser emission due to water molecules) appeared at 295 nm. All samples emitted in the range of 400–600 nm and showed a broad peak with a maximum at 480–490 nm. The wavelength position with maximum intensity was varied by ±5 nm. The intensities at the maximum wavelength varied seasonally and spatially, as shown in Figure 8.

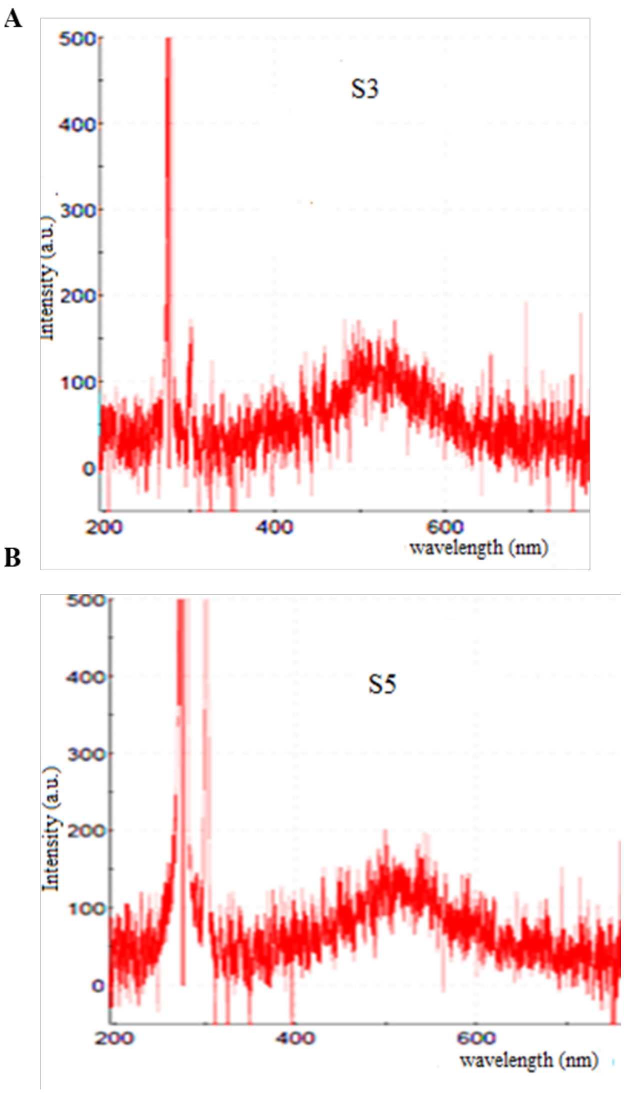

Figure 7. Emission spectra obtained from sampling sites (A) S3 and (B) S5 when excited at 266 nm.

Figure 8 shows that S1–S5 had similar concentrations of fluorescent substances. The intensities at S6 were remarkably lower than at the other five stations. It seems that the main road, which serves as a bridge, separates the wetland into two parts that behave differently. S1–S5 have different surrounding soils (Figure 2) that are less sandy than S6. Fluorescence intensities were generally higher during the dry season at S1–S5, except in January 2022. This seasonal pattern may reflect reduced dilution and increased concentration of dissolved organic matter during low-flow conditions, as well as enhanced sediment–water interactions in shallow areas.

3.6. Correlations between the variables

An exploratory multivariate statistical analysis was conducted to assess linear and monotonic relationships among the measured physicochemical parameters, nutrients, photosynthetic pigments, and fluorescence indices.[27–31] Both Pearson (r) and Spearman rank (ρ) correlation coefficients were calculated to assess linear and monotonic relationships, respectively, and to evaluate the robustness of the observed associations. Given the relatively small sample sizes for some variables and the presence of non-normal distributions, the results should be interpreted cautiously, with emphasis on relationships that are consistent across the two methods. Correlations that were statistically significant only in the Pearson analysis and not supported by Spearman coefficients were included for completeness but interpreted with caution.

Table 3 summarizes the statistically significant correlations, and the correlations for all parameters are shown in Table A3. The strongest positive relationship was observed between silicon and chl a ($r = 0.893$, $p = 0.001$; $\rho = 0.862$, $p = 0.003$). This result suggests an important role of silicon in phytoplankton biomass dynamics and productivity in the wetland.

A similarly strong and consistent negative correlation was found between total hardness and chl a ($r = -0.889$, $p = 0.001$; $\rho = -0.823$, $p = 0.006$), suggesting that increased ionic strength may limit phytoplankton growth (Table 3). In addition, total hardness was strongly negatively correlated with silicon ($r = -0.792$, $p = 0.011$; $\rho = -0.723$, $p = 0.028$), indicating potential geochemical controls on nutrient availability.

Chlorides exhibited a strong negative correlation with fluorescence emission intensity ($r = -0.835$, $p = 0.005$; $\rho = -0.733$, $p = 0.031$; Table 3), consistent across both methods and supporting the hypothesis that ionic strength influences fluorescence, potentially through quenching mechanisms.

The pH showed a strong positive correlation with total hardness ($r = 0.755$, $p = 0.019$; $\rho = 0.672$, $p = 0.047$) and a negative correlation with silicon ($r = -0.742$, $p = 0.022$; $\rho = -0.633$, $p = 0.076$) (Table 3). While the latter was slightly weaker in the Spearman analysis, the overall trend remained consistent.

Some correlations were statistically significant only in the Pearson analysis but not supported by Spearman coefficients (Table 3). For example, N-NH_4 showed a strong positive correlation with carotenoids ($r = 0.870$, $p = 0.002$), whereas the corresponding Spearman coefficient was lower and not statistically significant ($\rho = 0.559$, $p =$

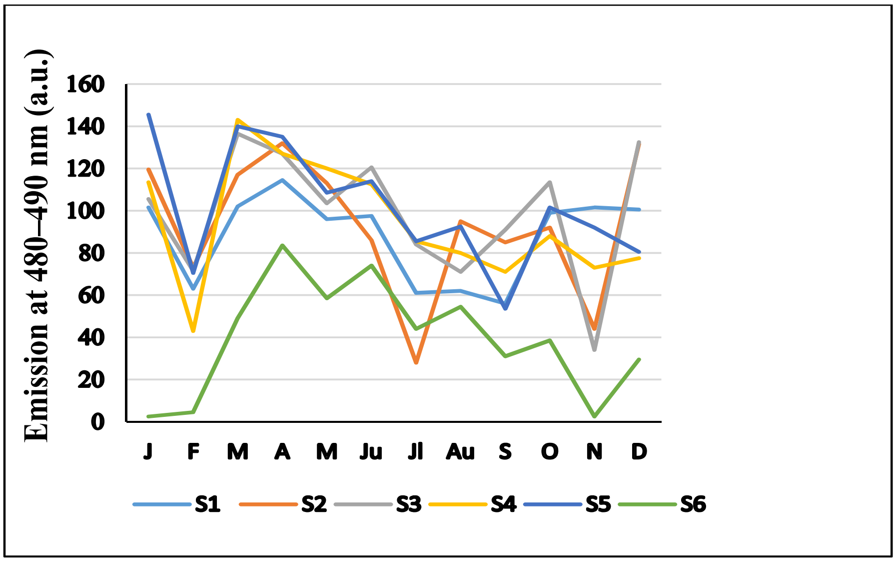

Figure 8. Monthly measurements of intensities from January to December 2022 at S1–S6 at Kalathas Wetland.

Table 3. Statistically significant correlations (Pearson's *r*, Spearman's ρ, and *p*-values)

Variables	Pearson *r*	*p*-value	Spearman ρ	*p*-value
Si–Chl a	0.893	0.001	0.862	0.003
Total hardness–Chl a	−0.889	0.001	−0.823	0.006
Chlorides–Fluorescence emission (480–490 nm)	−0.835	0.005	−0.733	0.031
Total hardness–Si	−0.792	0.011	−0.723	0.028
pH–Total hardness	0.755	0.019	0.672	0.047
pH–Si	−0.742	0.022	−0.633	0.076
P-PO_4–Si	−0.735	0.024	−0.463	0.209
NH_4–Chl a	0.699	0.036	0.621	0.074
Chl c–Carotenoids	−0.688	0.040	−0.617	0.086
NH_4–Carotenoids	0.870	0.002	0.559	0.117

0.117). This discrepancy suggests that the relationship may be influenced by skewed data distributions or a limited number of observations and should therefore be interpreted with caution.

Similarly, moderate correlations, such as N-NH_4 with chl a and P-PO_4 with silicon, showed weaker or non-significant Spearman correlations, indicating limited robustness of these associations. Overall, only correlations that are consistent across both Pearson and Spearman analyses are considered robust, while discrepancies between the two methods highlight the influence of non-normality and sample size limitations on the statistical relationships.

4. Discussion

4.1. Physicochemical parameters

The pH values indicated an alkaline water body (Tables A1 and A2). The electrical conductivity, salinity, and total hardness did not correlate consistently across the statistical analyses, suggesting strong spatial heterogeneity in the system.[32] Chloride did not show a statistically robust correlation with hardness (Table A3), indicating that other ions, such as sulfate (SO_4^{2-}) and bicarbonate (HCO_3^-), contribute significantly to salinity in the system.

As far as total hardness is concerned, generally it is due to bicarbonate ions (temporary or carbonate hardness) and to chloride and sulfate ions (permanent or non-carbonate hardness). In Kalathas Wetland, elevated total hardness values (Tables A1 and A2, Figure 5D) are likely associated with the geological structure of the study area, which is covered by Triassic–Cretaceous limestones, Miocene marls, and marly limestones (Figure 2). If only natural processes (soil type and geology) occur in a water body, bicarbonate ions are released into the water, and pH values correlate inversely with hardness and other physicochemical parameters. However, the observed positive relationships between pH and total hardness suggest that additional processes influence alkalinity. This may be attributed to anthropogenic inputs. As mentioned before, these include the construction of a road bridge and the disposal of quantities of construction materials containing limestone. However, alkalinity can be influenced by human activities, such as urbanization, liming, and fertilization.[33,34]

4.2. Nutrients and phytoplankton

In terms of macronutrients, silicon was the most abundant element compared to nitrogen and phosphorus. No statistically robust correlations were observed between nitrogen species and major ions (Table A3), potentially due to variability and limited sample size (Tables A1 and A2). This disagrees with strong correlations between ammonium and chloride, and between nitrate and chloride, that were found in a hypersaline, protected coastal wetland.[35] Both these nitrogen forms are available for algal growth, as is the phosphate. However, the statistical analysis did not reveal consistent relationships between nitrogen or phosphorus and phytoplankton biomass (Table A3), suggesting that these nutrients are not the primary limiting factors.

Generally, in coastal waters, the growth of larger phytoplankton species (such as diatoms) is affected by the content and composition of silicon.[36,37] This is strongly supported by the present results, which show that silicon exhibited a very strong and consistent positive correlation with chl a (Table 3), indicating its dominant role in controlling phytoplankton productivity. There are species, such as diatoms, that can grow in highly alkaline environments, but their metabolism is influenced by changes in carbonate chemistry, leading to their decline and dominance of other species such as dinoflagellates.[38] The growth and distribution of seaweeds are also influenced by salinity. Some species (e.g., brown algae) are either intolerant of high salinity or require lower bicarbonate (HCO_3) concentrations than are available.[39] However, bicarbonate ions account for a high percentage of the salinity in this wetland, as noted in the results section.

4.3. Pigments

The statistical analysis did not show consistent or robust relationships among carotenoids, chl b, and physicochemical parameters (Table A3), indicating that these pigments are influenced by multiple environmental factors rather than a single controlling variable. Carotenoids are components of diatoms, while chl a is a component of all photosynthetic algae and plants.[40]

Besides, the quantitative distribution of phytoplankton in many water systems can be estimated by comparing chlorophyll concentrations. When the concentration of chl c is greater than that of chl b, the diatoms are dominant.[40] This phenomenon was observed in our study.

4.4. Fluorescent compounds

Although not all the organic matter fluoresces, fluorescence remains a useful indicator of dissolved organic matter in water. From the literature, it is well known that fluorescence emission spectra consist of two peaks: one at 300–350 nm, corresponding to protein-like substances, and one at 450–500 nm, corresponding to humic-like substances.[9] Humic-like fluorophores are generally less intense than protein-like fluorophores. Protein-like fluorophores are due to anthropogenic pollution, while humic-like fluorophores are due to natural organic matter. Dissolved organic matter in marine coastal environments may also originate from phytoplankton.

The statistical analysis did not reveal consistent correlations between fluorescence and phytoplankton pigments (Table A3), suggesting that fluorescence is primarily associated with dissolved organic matter rather than biological production. In Kalathas Wetland, the LIF spectra of the water samples showed a broad peak with a maximum at 480–490 nm, indicating the presence of fluorescent compounds belonging to the humic category. The equivalent units in ppm qs were less than 24.7, with an average of 10.1 ppm qs units. In another coastal wetland in Crete that also used LIF, the qs units were below the LOD.[41] Most researchers have used conventional fluorescence, either by excitation-emission matrix spectroscopy or by synchronous spectroscopy, to standardize quinine sulfate units when excited at 350 nm rather than 266 nm. The concentrations in ppm qs that have been recorded range from 0.54 to 1.20 units in water with coastal phytoplankton species[42], 0.0154 units in estuarine water[43], and 4.3 units in rivers.[44] Therefore, the concentrations of fluorophores in Kalathas can be considered high and are mainly soil-derived. The stream suffers from illegal disposal of construction waste, including brick, clay tiles, plaster, and asphalt. Although these materials are typically not a threat to waterways[45], they may alter soil properties, thereby increasing the amount of fluorescent components in water. There is no previous knowledge of changes in soil properties and, consequently, in the fluorescence of wetlands, so this requires further investigation. However, a recent study has reported the presence of carbon nanoparticles in concrete, tiles, and plasterboard waste.[46] A strong and statistically significant negative correlation was observed between fluorescence emission and chloride concentration (Table 3), indicating that increasing ionic strength reduces fluorescence intensity. This is consistent with known quenching effects, as chloride ions can form non-fluorescent complexes.[47,48]

4.5. Comparison with other similar wetlands

To our knowledge, the only study on the water quality of Kalathas Wetland was conducted by our group in 2019.[49] The pH values are consistent, indicating that it is an alkaline water body. Moreover, statistical analyses showed only monthly fluctuations, with no spatial variation, while N-NH4 varied both spatially and monthly, with high values at most sites in February 2022 and lower values from June 2022 to the end of the sampling period. Silicon was the dominant nutrient, varying widely both spatially and monthly. Another agreement is that the S6 station had higher concentrations of salts (expressed as conductivity, total hardness, and salinity) compared with the other sites.

In India's Ganjam district, eight very small inland wetlands (0.01–1.5 km^2) were found to be influenced by anthropogenic pressure (primarily socioeconomic and demographic).[50] In that study, pollution was tracked using conventional chemical parameters and unconventional parameters such as nighttime light intensity and population density.

In Africa, a very small coastal wetland (only 0.7 km^2) studied showed severe anoxia and oxygen depletion due to the construction of a road bridge and to agricultural and recreational activities.[51]

In Spain, citizens were willing to pay for the conservation of a saline wetland, specifically to improve water quality and increase knowledge and awareness.[52]

4.6. Contributions

Based on the information provided in the paper, we highlight:

(i) Influence of natural processes and human activities: The results indicate that both natural processes and anthropogenic pressures shape the wetland's characteristics. The presence of humic-like substances and the influence of construction waste disposal suggest that human activities affect soil and water chemistry. In addition, hydrological modifications and marine intrusion contribute to the observed spatial variability, alongside natural seasonal changes.

(ii) Effectiveness of multivariate analysis and LIF in characterization: Multivariate statistical analysis identified key relationships among parameters, particularly the strong and consistent associations between silicon and chl a, total hardness and chl a, and chlorides and fluorescence. The combined use of Pearson and Spearman correlations improved the robustness of the analysis by accounting for non-normal data distributions. LIF effectively detected dissolved organic matter, indicating the presence of humic-like substances and providing complementary information on water quality. The interpretation of correlations may be influenced by temporal and spatial dependence among observations; therefore, longer time series would be required for more robust statistical inference.

(iii) Dominant nutrients influencing phytoplankton biomass: Among nitrogen, phosphorus, and silicon, silicon emerged as the dominant nutrient influencing phytoplankton productivity, showing a strong and consistent positive relationship with chl a. The phosphate and chl a concentrations indicate eutrophic conditions in the wetland. In contrast, nitrogen species did not show consistent relationships with phytoplankton biomass, suggesting that they are not the primary limiting factors in this system.

(iv) Contribution of geology: The geological setting influences soil properties, mineral composition, and geochemical processes, affecting nutrient availability and ionic composition. In particular, the presence of limestone formations contributes to elevated hardness and influences the overall physicochemical characteristics of the wetland.

(v) Implications for conservation and monitoring: The observed spatial and temporal variability in physicochemical parameters, nutrients, and fluorescence provides important insights for targeted monitoring and management. The strong influence of marine intrusion and localized anthropogenic inputs highlights areas that are particularly vulnerable to environmental pressures. Regular monitoring is therefore essential to detect changes in water quality and support effective conservation strategies for this sensitive coastal ecosystem.

5. Conclusion

The Kalathas Wetland in Crete, Greece, is a small but environmentally significant ecosystem currently exposed to multiple anthropogenic pressures. Despite its ecological importance and protected status, limited information exists regarding its environmental condition. The results demonstrated clear spatiotemporal variability in physicochemical parameters, nutrients, photosynthetic pigments, and fluorescence characteristics over the study period.

The wetland is characterized by alkaline conditions and strong spatial heterogeneity, particularly influenced by marine intrusion at S6. Among nutrients, silicon emerged as the dominant factor influencing phytoplankton biomass, exhibiting a strong and consistent positive relationship with chl a, while total hardness showed a strong negative association with chl a, suggesting that increased ionic strength may limit biological productivity. The phosphate and chl a concentrations are consistent with eutrophic conditions, whereas nitrogen species displayed high variability without robust relationships with phytoplankton biomass. Fluorescence analysis revealed the presence of humic-like substances, and the strong negative correlation between fluorescence intensity and chloride concentration indicates that ionic strength influences quenching. The combined use of Pearson and Spearman correlation analyses allowed the identification of robust relationships while highlighting the influence of non-normal distributions and limited sample size on weaker associations, supporting an exploratory interpretation of the results.

Overall, the findings indicate that water quality in Kalathas Wetland is affected by the combined effects of geological background, marine intrusion, and localized anthropogenic inputs. These results highlight the need for continuous, spatially targeted monitoring and management strategies to prevent further degradation and to support the long-term ecological sustainability of this vulnerable coastal ecosystem.

Acknowledgments

None.

Funding

This work was implemented in terms of the PhD studies of D-EZ. The publication fee was funded by the Hellenic Mediterranean University and the Public Investment Program of the Greek Ministry of Education and Religious Affairs under the project "Strengthening and optimizing the operation of MODY services and academic and research units of the Hellenic Mediterranean University," funded.

Conflict of interest

The authors declare they have no competing interests.

Author contributions

Conceptualization: Despoina-Eleni Zacharioudaki, Melina Kotti
Data curation: All authors
Formal analysis: All authors
Funding acquisition: All authors
Investigation: All authors
Methodology: All authors
Project administration: Melina Kotti
Resources: All authors
Software: All authors
Supervision: Melina Kotti
Validation: All authors
Visualization: Despoina-Eleni Zacharioudaki, Melina Kotti
Writing–original draft preparation: All authors
Writing–review and editing: All authors

Availability of data

The original contributions presented in this study are included in the article. Further inquiries can be directed to the corresponding author.

References

1. United Nations. No. 14583. Convention on wetlands of international importance especially as waterfowl habitat. Concluded at Ramsar, Iran, on February 2, 1971. Geneva, Switzerland: United Nations; 2001.

   doi: 10.18356/583cd2af-en-fr
2. Zotos A, Kokkoris IP, Charalampopoulos I, Bekri ES, Dimopoulos P. Wetlands in Crisis: The Silent Desertification Threat on the Greek Wetlands. *Land*. 2024;13(10):1567.

   doi: 10.3390/land13101567
3. Presidential Decree 2012. Government Gazette. 2012;229.
4. Water Framework Directive 2000/60/EC. Official Journal of the European Communities. 2000.
5. Hassan Omer N. Water Quality Parameters. Water Quality - Science, Assessments and Policy. July 2020.

   doi: 10.5772/intechopen.89657
6. Wetzel RG. *Limnology: Lake and River Ecosystems*. Academic Press, 2001.
7. Sene KJ, Farquharson FAK. Sampling Errors for Water Resources Design: The Need for Improved Hydrometry in Developing Countries. *Water Resour Manag*. 1998;12(2):121-138.

doi: 10.1023/a:1007952319495

8. Thomas JD. The role of dissolved organic matter, particularly free amino acids and humic substances, in freshwater ecosystems. *Freshw Biol*. 1997;38(1):1-36.

doi: 10.1046/j.1365-2427.1997.00206.x

9. Coble PG. Characterization of marine and terrestrial DOM in seawater using excitation-emission matrix spectroscopy. *Mar Chem*. 1996;51(4):325-346.

doi: 10.1016/0304-4203(95)00062-3

10. Baker A, Spencer RGM. Characterization of dissolved organic matter from source to sea using fluorescence and absorbance spectroscopy. *Sci Total Environ*. 2004;333(1-3):217-232.

doi: 10.1016/j.scitotenv.2004.04.013

11. Carstea EM, Ioja CI, Savastru R, Gavrilidis A. Spatial characterization of urban lakes. *Rom Rep Phys*. 2013;65(3):1092-1104.

12. Donard OFX, Lamotte M, Belin C, Ewald M. High-sensitivity fluorescence spectroscopy of Mediterranean waters using a conventional or a pulsed laser excitation source. *Mar Chem*. 1989;27(1-2):117-136.

doi: 10.1016/0304-4203(89)90031-5

13. Sharikova AV, Killinger DK. LIF detection of trace species in water using different UV laser wavelengths. *Int J High Speed Electron Syst*. 2007;17(4):689-695.

doi: 10.1142/S0129156407004898

14. World Wide Fund for Nature Greece. Inventory report: GR434KRI187—Kalathorema estuary. Ygrotopio Islands: Database of the Greek Island Wetlands. Published 2013.

15. Fytrolakis N. *The Geological Structure of Crete* (in Greek). Dissertation. National Technical University of Athens. 1980.

16. Kokinou E, Sarris A. Detection of the near surface structure through a multidisciplinary approach. *Cent Eur J Geosci*. 2011;3(4):349-357.

doi: 10.2478/s13533-011-0034-2

17. American Public Health Association, American Water Works Association, Water Environment Federation. *Standard Methods for the Examination of Water and Wastewater*. 21st ed. American Public Health Association; 2005.

18. Lawson-Wood K, Evans K. *Determination of Quinine in Tonic Water Using Fluorescence Spectroscopy*. Application Note. Seer Green, United Kingdom: PerkinElmer; 2018.

19. Organisation for Economic Co-operation and Development. *Eutrophisation des eaux: méthodes de surveillance, d'évaluation et de lutte* [*Eutrophication of Waters: Monitoring, Assessment and Control Methods*]. Paris, France: Organisation for Economic Co-operation and Development; 1982:164.

20. Correll D. Phosphorus: a rate limiting nutrient in surface waters. *Poult Sci*. 1999;78(5):674-682.

doi: 10.1093/ps/78.5.674

21. Schlesinger WH. *Biogeochemistry*. 2nd ed. Academic Press; 1997.

22. Sen B, Alp MT, Sönmez F, Mehmet K, Özgür C. Relationship of algae to water pollution and wastewater treatment. In: Elshorbagy W, Chowdhury RK, eds. *Water Treatment*. London, United Kingdom: InTech; 2013.

doi: 10.5772/51927

23. Al-Thani JA, Soliman Y, Al-Maslamani IA, Yigiterhan O, Al-Ansari EMAS. Physical drivers of chlorophyll and nutrients variability in the Southern-Central Arabian Gulf. *Estuar Coast Shelf Sci*. 2023;283:108260.

doi: 10.1016/j.ecss.2023.108260

24. Walsham P, Aminot A, Rey F, *et al*. *Determination of Chlorophyll in Seawater*. ICES Techniques in Marine Environmental Science (TIMES); København, Denmark: International Council for the Exploration of the Sea; 2022.

doi: 10.17895/ICES.PUB.20207798

25. Sournia A. *Phytoplankton Manual*. Geneva, Switzerland: United Nations Educational, Scientific and Cultural Organization; 1978:337.

26. Parsons TR, Maita Y, Lalli CM. *A Manual of Chemical and Biological Methods for Seawater Analysis*. Oxford, UK: Pergamon Press; 1984:173.

27. Aggarwal CC, Reddy CK. *Data Clustering: Algorithms and Applications*. Boca Raton, FL, USA: Chapman & Hall; 2013.

28. Anderson TW. *An Introduction to Multivariate Statistical Analysis*. 3rd ed. Hoboken, NJ, USA: John Wiley & Sons; 2003.

29. Draper NR, Smith H. *Applied Regression Analysis*. 3rd ed. Hoboken, NJ, USA: John Wiley & Sons; 1998.

30. Everitt BS, Landau S, Leese M, Stahl D. *Cluster Analysis*. 5th ed. Hoboken, NJ, USA: John Wiley & Sons; 2011.

31. Hotelling H. Relations between two sets of variates. *Biometrika*. 1936;28:321-377.

doi: 10.2307/2333955

32. Kokinou E, Zacharioudaki DE, Kokolakis S, *et al*. Spatiotemporal environmental monitoring of the karst-related Almyros Wetland (Heraklion, Crete, Greece, Eastern Mediterranean). *Environ Monit Assess*. 2023;195(8).

doi: 10.1007/s10661-023-11571-5

33. Raymond PA, Cole JJ. Increase in the export of alkalinity from North America's largest river. *Science*. 2003;301(5629):88-91.

doi: 10.1126/science.1083788

34. Kaushal SS, Likens GE, Utz RM, Pace ML, Grese M, Yepsen

M. Increased river alkalinization in the Eastern US. *Environ Sci Technol.* 2013;47(18):10302-10311.

doi: 10.1021/es401046s

35. Samara F, Knuteson SL, Abdulateef TA, *et al.* Assessment and Management of the Water Quality and Heavy-Metal Pollution of a Protected Hypersaline Wetland in the United Arab Emirates. *Water*. 2023;15(9):1766.

    doi: 10.3390/w15091766

36. Lindsey R, Scott M. What are phytoplankton? *NASA Earth Observatory*. Published 2010. Available from: http://earthobservatory.nasa.gov/Features/Phytoplankton [Last accessed on June 23, 2025].

37. National Oceanic and Atmospheric Administration. Phytoplankton. Ocean Facts. 2021. Available from: https://oceanservice.noaa.gov/facts/phyto.html [Last accessed on June 23, 2025].

38. Keys M, Highfield A, Chrachri A, Ostle C, Brownlee C, Wheeler GL. Dynamic changes in phycosphere carbonate chemistry reveal rapid modulation of carbon uptake in single diatom cells. *Sci Adv*. 2026;12(1).

    doi: 10.1126/sciadv.ady8646

39. Li J, Liu Y, Liu Y, Wang Q, Gao X, Gong Q. Effects of temperature and salinity on the growth and biochemical composition of the brown alga *Sargassum fusiforme* (Fucales, Phaeophyceae). *J Appl Phycol.* 2019;31:3061-3068.

    doi: 10.1007/s10811-019-01795

40. Cirenko LA. The information value of chlorophyll index. *Hydro Biol.* 1980;4(24):49 -53.

41. Zacharioudaki DE, Fitilis I, Kotti M. Application of laser-induced fluorescence for characterization of water quality in two wetlands. In: Proceedings of the 4th International Conference in Electronic Engineering, Information Technology & Education (EEITE 2023). May 15–19, 2023; Chania, Greece.

42. Fukuzaki K, Imai I, Fukushima K, Ishii KI, Sawayama S, Yoshioka T. Fluorescent characteristics of dissolved organic matter produced by bloom-forming coastal phytoplankton. *J Plankton Res*. 2014;36(3):685-694.

    doi: 10.1093/plankt/fbu015

43. Boehme JR, Coble PG. Characterization of Colored Dissolved Organic Matter Using High-Energy Laser Fragmentation. *Environ Sci Technol*. 2000;34(15):3283-3290.

    doi: 10.1021/es9911263

44. Chen Z, Wen Y, Xiao M, Yue F, Zhang W. Characteristics of Dissolved Organic Matter Impacted by Different Land Use in Haihe River Watershed, China. *Int J Environ Res Public Health*. 2023;20(3):2432.

    doi: 10.3390/ijerph20032432

45. Musarat MA, Alaloul WS, Qureshi AH, Ghufran M. Construction waste to energy: technologies, economics, and challenges. In: Rahimpour MR, ed. *Encyclopedia of Renewable Energy*, *Sustainability and the Environment*. Elsevier; 2024:51-60.

46. Oliveira MLS, Izquierdo M, Querol X, Lieberman RN, Saikia BK, Silva LFO. Nanoparticles from construction wastes: A problem to health and the environment. *J Clean Prod.* 2019;219:236-243.

    doi: 10.1016/j.jclepro.2019.02.096

47. Babko AK, Kostyshina AP. Quenching of the luminescence of quinine sulfate and rhodamine dyes in solutions. *Ukr Khim Zh*. 1969;35:544-551.

48. Eisenbrand J, Raisch M. Beiträge zur Fluorimetrie. *Z Anal Chem*. 1961;179:352-355.

49. Giannoudakis N, Zacharioudaki DE, Kotti M. Variations of physicochemical parameters and photosynthetic pigments in a small-sized wetland in the prefecture of Chania, Greece. In: Proceedings of the 4th International Conference in Electronic Engineering, Information Technology & Education (EEITE 2023*)*. May 15–19, 2023; Chania, Greece.

50. Pattnayak SP, Jena P, Roul P, Gulab SK, Prusty BAK. Water quality surveillance of small inland wetlands integrating multi-dimensional drivers. *Appl Water Sci*. 2025;16(1).

    doi: 10.1007/s13201-025-02672-2

51. Newton A, Icely J, Cristina S, *et al*. Anthropogenic, Direct Pressures on Coastal Wetlands. *Front Ecol Evol*. 2020;8.

    doi: 10.3389/fevo.2020.00144

52. Soliño-Barreiro C, Jiménez-Espinosa R, Soliño M. The Social Relevance of Water Quality and Cultural Ecosystem Services: An Application to a Saline Wetland in an Arid Environment. *Aquat Conserv.* 2025;35(5).

    doi: 10.1002/aqc.70146

Appendix

Table A1. Descriptive statistics with outliers

Variable	*n*	Mean	SD	IQR	Skewness	Min.	Max.
pH	72	8.238	0.561	0.477	−1.252	5.930	9.390
Salinity (‰)	72	9.244	6.358	4.575	1.252	0.300	35.300
Conductivity (mS/cm)	72	13.02	6.488	5.297	0.071	0.800	26.200
Chlorides (mg/L)	72	16,650	4,719	5,453	0.207	7,090	28,720
Hardness (mg/L)	72	1,627	1,094	1,025	1.749	160	6,520
N-NH_4 (mg/L)	52	0.348	0.550	0.197	3.076	0.029	2.614
N-NO_3 (mg/L)	65	0.410	0.266	0.369	0.359	0	1.163
P-PO_4 (mg/L)	48	0.064	0.044	0.074	0.071	0.009	0.130
Si (mg/L)	58	2.463	1.924	2.747	0.976	0	9.000
Chl a (μg/L)	64	16.460	10.62	17.430	0.278	0	40.430
Chl b (μg/L)	45	11.440	9.248	16.300	0.534	0	29.500
Chl c (μg/L)	70	15.140	9.298	15.580	0.208	0	37.340
Carotenoids (μg/L)	30	4.927	6.538	5.225	3.577	0.257	35.050
Fluorescence emission (480–490 nm)	72	85.920	34.640	50.380	−0.480	2.50	145.500

Abbreviations: Chl: Chlorophyll; IQR: Interquartile range; SD: Standard deviation.

Table A2. Descriptive statistics without outliers

Variable	*n*	Mean	SD	IQR	Skewness	Min.	Max.
pH	63	8.287	0.305	0.400	0.171	7.670	8.960
Chlorides (mg/L)	63	16,870	4,540	5,268	0.203	7,090	28,720
Hardness (mg/L)	63	1,693	1,135	775	1.659	160	6,520
N-NH_4 (mg/L)	46	0.367	0.581	0.180	2.872	0.029	2.614
N-NO_3 (mg/L)	57	0.368	0.233	0.398	−0.053	0	0.746
P-PO_4 (mg/L)	44	0.065	0.045	0.090	0.012	0.009	0.130
Si (mg/L)	52	2.353	1.698	2.714	0.543	0	7.088
Chl a (μg/L)	56	16.820	11.040	18.300	0.218	0	40.430
Chl b (μg/L)	37	11.740	8.778	15.420	0.353	0	26.720
Chl c (μg/L)	62	16.030	9.215	15.680	0.078	0	37.340
Carotenoids (μg/L)	27	5.238	6.824	5.566	3.401	0.257	35.050
Fluorescence emission (480–490 nm)	63	83.870	33.780	44.500	−0.313	2.500	143.000

Abbreviations: Chl: Chlorophyll; IQR: Interquartile range; SD: Standard deviation.

Table A3. Correlation table

Correlation parameters		Pearson		Spearman	
1	2	*r*	*p*	ρ	*p*
pH	Chlorides (mg/L)	−0.261	0.497	−0.183	0.644
pH	Hardness (mg/L)	0.755	0.019*	0.672	0.047*
pH	$N\text{-}NH_4$ (mg/L)	−0.189	0.625	−0.322	0.398
pH	$N\text{-}NO_3$ (mg/L)	−0.646	0.060	−0.417	0.270
pH	$P\text{-}PO_4$ (mg/L)	0.620	0.075	0.332	0.382
pH	Si (mg/L)	−0.742	0.022*	−0.633	0.076
pH	Chl a (μg/L)	−0.576	0.105	−0.561	0.116
pH	Chl b (μg/L)	0.018	0.963	0.100	0.810
pH	Chl c (μg/L)	−0.057	0.884	−0.067	0.880
pH	Carotenoids (μg/L)	−0.002	0.996	−0.050	0.912
pH	Fluorescence emission (480–490 nm)	−0.013	0.974	−0.283	0.463
Chlorides (mg/L)	Hardness (mg/L)	0.253	0.511	0.235	0.542
Chlorides (mg/L)	$N\text{-}NH_4$ (mg/L)	−0.587	0.097	−0.288	0.452
Chlorides (mg/L)	$N\text{-}NO_3$ (mg/L)	0.269	0.484	0.083	0.843
Chlorides (mg/L)	$P\text{-}PO_4$ (mg/L)	−0.518	0.153	−0.358	0.343
Chlorides (mg/L)	Si (mg/L)	0.166	0.670	0.300	0.437
Chlorides (mg/L)	Chl a (μg/L)	−0.119	0.761	0.092	0.814
Chlorides (mg/L)	Chl b (μg/L)	−0.137	0.725	0.100	0.810
Chlorides (mg/L)	Chl c (μg/L)	0.288	0.453	0.000	1.000
Chlorides (mg/L)	Carotenoids (μg/L)	−0.658	0.054	0.133	0.744
Chlorides (mg/L)	Fluorescence emission (480–490 nm)	−0.835	0.005**	−0.733	0.031*
Hardness (mg/L)	$N\text{-}NH_4$ (mg/L)	−0.666	0.050	−0.402	0.284
Hardness (mg/L)	$N\text{-}NO_3$ (mg/L)	−0.232	0.549	−0.235	0.542
Hardness (mg/L)	$P\text{-}PO_4$ (mg/L)	0.323	0.396	−0.066	0.866
Hardness (mg/L)	Si (mg/L)	−0.792	0.011*	−0.723	0.028*
Hardness (mg/L)	Chl a (μg/L)	−0.889	0.001**	−0.823	0.006**
Hardness (mg/L)	Chl b (μg/L)	−0.156	0.689	−0.353	0.351
Hardness (mg/L)	Chl c (μg/L)	0.374	0.322	0.269	0.484
Hardness (mg/L)	Carotenoids (μg/L)	−0.626	0.072	−0.092	0.813
Hardness (mg/L)	Fluorescence emission (480–490 nm)	−0.252	0.513	−0.437	0.240
$N\text{-}NH_4$ (mg/L)	$N\text{-}NO_3$ (mg/L)	−0.131	0.738	−0.170	0.663
$N\text{-}NH_4$ (mg/L)	$P\text{-}PO_4$ (mg/L)	−0.116	0.766	−0.285	0.458
$N\text{-}NH_4$ (mg/L)	Si (mg/L)	0.382	0.311	0.424	0.256
$N\text{-}NH_4$ (mg/L)	Chl a (μg/L)	0.699	0.036*	0.621	0.074
$N\text{-}NH_4$ (mg/L)	Chl b (μg/L)	−0.161	0.679	−0.458	0.215
$N\text{-}NH_4$ (mg/L)	Chl c (μg/L)	−0.346	0.362	−0.017	0.965
$N\text{-}NH_4$ (mg/L)	Carotenoids (μg/L)	0.870	0.002**	0.559	0.117
$N\text{-}NH_4$ (mg/L)	Fluorescence emission (480–490 nm)	0.332	0.383	0.153	0.695

(*Cont'd...*)

Table A3. (***Continued***)

Correlation parameters		Pearson		Spearman	
1	2	*r*	*p*	ρ	*p*
N-NO_3 (mg/L) 2	P-PO_4 (mg/L)	−0.649	0.059	−0.507	0.163
N-NO_3 (mg/L) 2	Si (mg/L)	0.479	0.192	0.350	0.359
N-NO_3 (mg/L) 2	Chl a (μg/L)	0.150	0.700	0.017	0.966
N-NO_3 (mg/L) 2	Chl b (μg/L)	−0.061	0.877	0.217	0.581
N-NO_3 (mg/L) 2	Chl c (μg/L)	0.512	0.158	0.467	0.213
N-NO_3 (mg/L) 2	Carotenoids (μg/L)	−0.468	0.204	−0.550	0.133
N-NO_3 (mg/L) 2	Fluorescence emission (480–490 nm)	−0.114	0.769	−0.150	0.708
P-PO_4 (mg/L)	Si (mg/L)	−0.735	0.024*	−0.463	0.209
P-PO_4 (mg/L)	Chl a (μg/L)	−0.478	0.193	−0.123	0.753
P-PO_4 (mg/L)	Chl b (μg/L)	0.480	0.191	0.446	0.229
P-PO_4 (mg/L)	Chl c (μg/L)	−0.463	0.210	−0.586	0.097
P-PO_4 (mg/L)	Carotenoids (μg/L)	0.253	0.511	0.227	0.556
P-PO^4 (mg/L)	Fluorescence emission (480–490 nm)	0.480	0.191	0.533	0.139
Si (mg/L)	Chl a (μg/L)	0.893	0.001**	0.862	0.003**
Si (mg/L)	Chl b (μg/L)	0.048	0.902	0.200	0.613
Si (mg/L)	Chl c (μg/L)	0.006	0.987	0.000	1.000
Si (mg/L)	Carotenoids (μg/L)	0.227	0.557	0.150	0.708
Si (mg/L)	Fluorescence emission (480–490 nm)	−0.223	0.565	−0.233	0.552
Chl a (μg/L)	Chl b (μg/L)	0.119	0.761	0.259	0.500
Chl a (μg/L)	Chl c (μg/L)	−0.279	0.467	−0.209	0.589
Chl a (μg/L)	Carotenoids (μg/L)	0.624	0.072	0.385	0.306
Chl a (μg/L)	Fluorescence emission (480–490 nm)	−0.066	0.865	0.042	0.915
Chl b (μg/L)	Chl c (μg/L)	−0.323	0.397	−0.200	0.613
Chl b (μg/L)	Carotenoids (μg/L)	0.117	0.764	−0.250	0.521
Chl b (μg/L)	Fluorescence emission (480–490 nm)	0.083	0.833	−0.033	0.948
Chl c (μg/L)	Carotenoids (μg/L)	−0.688	0.040*	−0.617	0.086
Chl c (μg/L)	Fluorescence emission (480–490 nm)	−0.104	0.790	−0.133	0.744
Carotenoids (μg/L)	Fluorescence emission (480–490 nm)	0.373	0.323	−0.067	0.880

Notes: * $p < 0.05$, ** $p < 0.01$.
Abbreviation: Chl: Chlorophyll.